Part III

ELECTROCARDIOGRAPHY IN PULMONARY HYPERTENSION

Chapter 9

DETECTION OF ELEVATED PULMONARY PRESSURES BY THE ECG-DERIVED VENTRICULAR GRADIENT: A COMPARISON OF CONVERSION MATRICES IN PATIENTS WITH SUSPECTED PULMONARY HYPERTENSION

Marlieke L.A. Haeck*
Gijsbert F.L. Kapel GFL*
Roderick W.C. Scherptong
Cees A. Swenne
Aire C. Maan
Jeroen J. Bax
Martin J. Schalij
Hubert W. Vliegen

*Both authors contributed equally to this work

Submitted

ABSTRACT

Background

The aim was to assess the diagnostic value of the Inverse Dower (INVD)-derived vectorcardiogram (VCG) and the Kors-derived VCG to detect elevated systolic pulmonary arterial pressure (SPAP) in suspected pulmonary hypertension.

Methods

In 132 patients, morphologic variables were evaluated by comparing the VCG parameters synthesized by INVD and Kors matrix. Comparison of the diagnostic accuracy of detecting SPAP≥50 mm Hg between the matrices was performed by ROC curve analysis and logistic regression analysis.

Results

Most VCG parameters differed significantly between INVD and Kors. ROC analysis for detection of SPAP≥50 mm Hg by VG projected on the X-axis demonstrated no difference (p=0.99) between INVD (AUC=0.80) and Kors (AUC=0.80). Both matrices yielded significant diagnostic information on the presence of SPAP≥50 mm Hg (INVD, OR 1.05, 95%CI 1.03–1.07; *P*<0.001; Kors, OR 1.05, 95%CI 1.03–1.08; *P*<0.001).

Conclusion

Although there were significant differences in vector morphology, both INVD- and Kors-derived VCG demonstrated equal clinical performance in case of elevated SPAP.

INTRODUCTION

Pulmonary hypertension (PH) is a severe and progressive disease in which timely detection is necessary to improve prognosis.[1-3] Therefore, a simple and noninvasive test to detect PH is warranted. The ECG-derived vectorcardiogram (VCG) was demonstrated to have high diagnostic accuracy for detecting elevated pulmonary pressures in patients with idiopathic pulmonary arterial hypertension and in patients with suspected PH.[4,5] The ECG is widely available and, therefore the ECG-derived VCG could be a valuable tool in screening patients at risk for developing PH. The ECG-derived VCG is constructed from the conventional 12-lead ECG with the use of a conversion matrix.[6,7] Edenbrandt et al. developed the INVD matrix by reversing the Dower matrix, originally used for VCG-to-ECG conversion, and based on an anatomical model.[6,8,9] Thereafter, Kors et al. improved the ECG-to-VCG conversion by designing a new matrix.[7] Nowadays, the Kors matrix is the most widely used matrix. Previous studies, demonstrating the value of the VCG in detecting elevated pulmonary pressures in PH, used the INVD matrix.[4,5] However, it remains unknown what the impact of the VCG synthesis algorithm is on the diagnostic accuracy of the VCG to diagnose PH.

Therefore the aims of the current study were to evaluate the morphologic differences between the VCG synthesized by the INVD matrix and the Kors matrix and to assess the diagnostic value of both matrices to detect elevated pulmonary pressure in patients with suspected PH.

METHODS

Study population

Patients referred to the outpatient clinic for PH screening were evaluated. As part of the non-invasive screening protocol for PH, all patients underwent echocardiography in order to estimate the systolic pulmonary arterial pressure (SPAP). The presence of pulmonary hypertension was considered likely in case of SPAP ≥36 mm Hg and very likely in case of SPAP ≥50 mm Hg.[10] In addition, an ECG was obtained to screen for common patterns associated with RV hypertrophy.[10] This ECG was subsequently synthesized into a VCG and analyzed using dedicated software. Furthermore, functional class according to the New York Heart Association (NYHA) was determined for all patients. Data were prospectively collected in the departmental Cardiology Information System (EPD-Vision®, Leiden University Medical Centre, The Netherlands) and were retrospectively analyzed. Patients were included if an ECG was available within 90 days of echocardiography and if SPAP was measurable. Furthermore, patients with a systemic right ventricle (RV), pacemaker, atrial fibrillation at time of ECG or previous myocardial infarction were excluded.

Electrocardiography

ECGs were recorded with standard electrocardiographs and processed by the ECG Analysis Program of the University of Glasgow.[11] The electronically stored ECGs were exported from the ECG database management system and analyzed with the MATLAB-based (The MathWorks, Natick, MA) computer program LEADS (Leiden the Netherlands).[12] LEADS derives the VCG from the standard ECG using a predefined conversion matrix.[12]

LEADS first identifies the QRS-complexes and adjusts for variations of the baseline. Thereafter, beats were automatically selected based on the signal to noise ratio, variability of the interbeat

interval time and consistency of the morphology of the QRS-T complexes. This automated selection was reviewed by the analyst, who could manually adjust the selection to obtain representative beats. Secondly, the selected beats were averaged into one QRST complex, which was subsequently synthesized into an average VCG complex using a predefined conversion matrix. For the purpose of the current study, the average VCG complex was synthesized using both the Inverse Dower (INVD) matrix and the Kors matrix.[6,7] After conversion, LEADS detects the QRS onset, the J point and the end of the T-wave.[13]

Finally, the landmarks in time were used to calculate the magnitude and orientation of the mean QRS-vector and T-vector. Orientations were defined by azimuth and elevation, according to the American Heart Association vectorcardiography coordinates standard.[14] Furthermore, the x, y, and z-deflections of the QRS-complex and T-wave were divided in 2 ms intervals from which the area under the complex is approximated. The areas under the complex of the intervals were added to calculate the integral of the QRS-complex (QRS-integral) and T-wave (T-integral).

The QRS-integral and T-integral were both used to compute the QRST spatial angle and the ventricular gradient (VG) magnitude and orientation, including the VG projected on the x-axis (VGx; Figure 1).[15] In previous studies it was demonstrated that a VGx of 24 mV*ms is the lower limit of a normal VGx and that VGX< 24 mV*ms was associated with the presence of PH.[4,5]

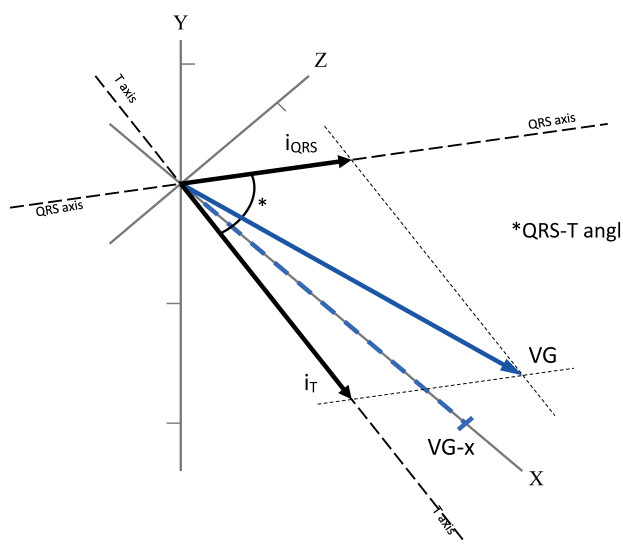

Figure 1. Orientations of cardiac vectors. IQRS and IT, the thick black arrows, are the integrals of respectively the QRS- and T-vector, which have the same orientation as the QRS and T axes. The angle between the QRS and the T axes is the QRS-T spatial angle. VG indicates the ventricular gradient vector, which is the resultant of the integrals of the QRS- and T-vector. Right ventricular overload, as a consequence of elevated pulmonary pressures, causes a change in the magnitude and orientation of the QRS-, T-, and VG-vector. In a study by Scherptong et al.[5], the VG projected on the x-axis (VGx), denoted as the thick blue dashed line on the x-axis, correlated the strongest with the elevated pulmonary pressures as compared to other VCG parameters in a heterogeneous population suspected of PAH. VGx and elevated pulmonary pressures were inversely correlated, hence increased pulmonary pressures caused a decreased VGx.[5]

Echocardiography

Patients were examined in left lateral decubitus position with a commercially available echocardiography system (Vivid Seven or E9, General Electric, Milwaukee, Wisconsin). The SPAP was calculated by adding RV pressure to the right atrial pressure. RV pressure was estimated by calculating the maximum velocity of the tricuspid regurgitant jet using the modified Bernoulli equation. The right atrial pressure was estimated based on the diameter and inspiratory collapse of the vena cava inferior.[16]

Statistical analysis

Continuous data were reported as mean ± standard deviation and categorical data as frequencies and percentages. The patient population was divided into three groups based on the SPAP: < 36 mm Hg, 36 – 49 mm Hg and ≥ 50 mm Hg. Patient characteristics were compared using the one-way analysis of variance test or χ^2 test. The matrices INVD and Kors were compared for all VCG parameters by a paired student *t* test. The mean difference and standard deviation between INVD and Kors matrices were calculated for all VCG parameters, by subtracting Kors from INVD. In addition, to visualize the distribution and evaluate the magnitude of the differences between the INVD and Kors matrices, Bland Altman plots were drawn for the integrals of the QRS- and T-vector, VG magnitude and VGx. To compare the measure for agreement between INVD and Kors measuring the same variable, the mean and 2 x SD of the difference between INVD and Kors was determined in the Bland Altman plots.[17] In addition, the correlation coefficient between both matrices was calculated for the QRS- and T-vector, VG magnitude and VGx. The Pearson correlation was used to determine the correlation coefficient between the VCG parameters and the SPAP, estimated with echocardiography, for both matrices.

To determine the discrepancy in diagnostic accuracy between the INVD and Kors matrices for the detection of elevated pulmonary pressures (SPAP ≥ 36 mm Hg and SPAP ≥ 50 mm Hg), by VGx, the areas under the curve (AUC) of the receiver operator characteristic (ROC) curve were compared. The method by Hanley and McNeil, which accounts for the concordance between two measurements of the same subjects, was used to compare the AUC of the INVD and Kors matrices.[18]

Thereafter, the association between elevated SPAP (≥ 36 and ≥ 50 mm Hg) and the VGx as continuous and dichotomous variable found in previous studies (VGx <24 mV*ms)[4,5] was investigated for both matrices using univariable logistic regression analysis. Thereafter, the odds ratios were corrected for age, gender and heart rate to obtain the multivariate odds ratios. A *P*-value <0.05 were considered statistically significant. SPSS software (20.0, SPSS Inc, Chicago, USA) was used for all statistical analyses.

RESULTS

Patients characteristics

A total of 132 patients was included in the study. Patient characteristics are summarized in Table 1. The mean age was 54 ± 15 years, 36% (n=47) was male and the mean SPAP was 43 ± 21 mm Hg. Twenty-five patients had moderately elevated pulmonary pressures (SPAP ≥36 mm Hg) and 46 patients had severely elevated pulmonary pressures (SPAP ≥50 mm Hg), the remaining 61 patients had SPAP

<36 mm Hg. There was no significant difference in sex, heart rate or body surface area between the three patient groups. However, patients with SPAP ≥36 and <50 mm Hg were older compared to the normal SPAP group and patients with SPAP ≥50 mm Hg had more impaired functional class than patients with SPAP <36 mm Hg (Table 1).

Table 1. Patient Characteristics

Clinical characteristics	Total population (n=132)	SPAP <36 mm Hg (n=61)	SPAP 36 - 49 mm Hg (n=25)	SPAP ≥ 50 mm Hg (n=46)	*P*-value
Age (years)	54 ± 15	49 ± 15	59 ± 13*	57 ± 15*	0.003
Male	47 (36)	19 (31)	10 (40)	18 (39)	0.61
NYHA functional class	2.2 ± 0.8	2.0 ± 0.8	2.1 ± 0.7	2.5 ± 0.7*	0.003
Heart rate (beats/min)	75 ± 14	73 ± 13	75 ± 15	78 ± 16	0.25
BSA (m^2)	1.8 ± 0.2	1.9 ± 0.2	1.8 ± 0.2	1.8 ± 0.2	0.55
Echocardiography					
Estimated SPAP (mm Hg)	43 ± 21	26 ± 4	43 ± 4*	66 ± 18*	<0.001

* *P*<0.05 compared to SPAP<36 mm Hg.
BSA, body surface area; NYHA, New York Heart Association; PH, pulmonary hypertension; SPAP, systolic pulmonary arterial pressure

The differences between the Inverse Dower en Kors matrices

VCG parameters are listed in Table 2. The magnitude of the mean QRS-vector synthesized by the INVD matrix (350 ± 164 μV) was larger as compared to the magnitude of the mean QRS-vector synthesized by the Kors matrix (329 ± 153 μV). Furthermore, the Kors derived QRS-vector was directed more anterior (azimuth, 8 ± 66° vs. 27 ± 67°) and superior (elevation, 21 ± 29° vs. 17 ± 30°) as compared to the INVD derived QRS-vector. The mean T-vector magnitude of the INVD reconstructed VCG (156 ± 85 μV) was comparable with the mean T-vector magnitude of the Kors reconstructed VCG (154 ± 76 μV), however, the orientation of the Kors derived T-vector was more superior (elevation, 24 ± 19° vs. 18 ± 21°) compared to the INVD derived T-vector. The QRST spatial angle, the angle between the QRS- and T-vector, was significantly wider when the VCG was derived by the INVD matrix (87 ± 37°) in comparison to the Kors matrix (76 ± 41°).

The magnitude of the integral of the QRS-vector obtained using the INVD matrix was significantly larger as compared to the magnitude of the integrals of the QRS- vector obtained using the Kors matrix (32 ± 17 vs. 30 ± 16 μV). However, the magnitude of the integral of the T-vector was comparable between the two matrices. The Bland Altman plots of the integrals of these vectors demonstrated a small mean difference between both matrices, however a large variation in these differences was observed (Figures 2A and 2B). The integrals of the T- and QRS-vectors derived by the INVD matrix correlated well with the integrals of the T- and QRS-vectors derived by the Kors matrix (r=0.95, *P*<0.001; r=0.97, *P*<0.001, respectively).

A small, but significant difference in the VG magnitude was observed between the Kors and INVD matrices (Figure 2C; 54 ± 25 mV·ms vs. 57 ± 25 mV·ms). As expected, since the VG is the resultant

Table 2. Vectorcardiographic characteristics of the inverse Dower and Kors matrices

	INVD	Kors	Difference INVD - Kors	Paired T-test (*P*-value)
QRS mean (μV)	350 ± 164	329 ± 153	22 ± 62	<0.001
QRS axis azimuth (°)	27 ± 67	8 ± 66	9 ± 28	0.001
QRS elevation (°)	17 ± 30	21 ± 29	-4 ± 9	<0.001
QRS integral (mV*ms)	32 ± 17	30 ± 16	2 ± 6	0.002
T mean (μV)	156 ± 85	154 ± 76	2 ± 24	0.28
T axis azimuth (°)	-26 ± 55	-26 ± 48	0.2 ± 23	0.93
T axis elevation (°)	18 ± 21	24 ± 19	-6 ± 7	<0.001
T integral (mV*ms)	47 ± 21	47 ± 19	0.3 ± 6	0.53
QRS-T angle (°)	87 ± 37	76 ± 41	11 ± 18	<0.001
Ventricular gradient magnitude (mV*ms)	54 ± 25	57 ± 25	-3 ± 7	<0.001
Ventricular gradient azimuth (°)	2 ± 47	-4 ± 41	8 ± 22	0.07
Ventricular gradient elevation (°)	25 ± 23	29 ± 23	-4 ± 7	<0.001
VGx (mV*ms)	36 ± 27	39 ± 25	-3 ± 6	<0.001

INVD, inverse Dower matrix; VGx, ventricular gradient projected on the x-axis

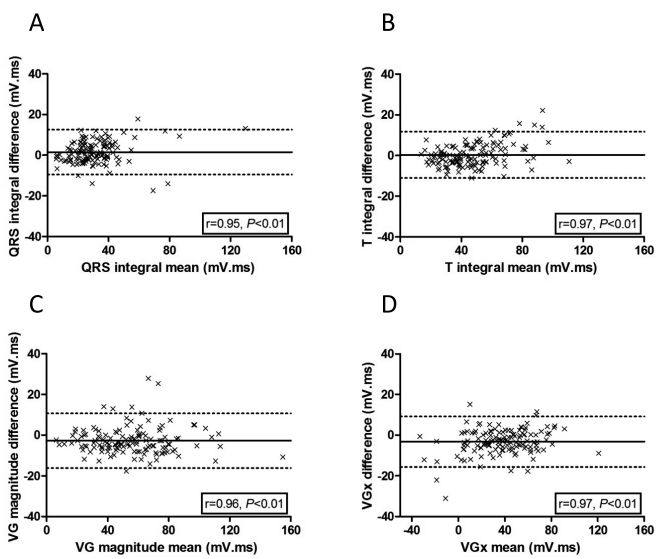

Figure 2. Bland Altman plots for the differences between the inverse Dower and Kors matrices by subtracting the KORS-derived VCG from the INVD-derived VCG. Panel A depicts the QRS integral, panel B depicts the integral of the T vector, panel C depicts the ventricular gradient and panel D depicts the ventricular gradient projected on the x-axis. VG: ventricular gradient; VGx: ventricular gradient projected on the x-axis.

of the QRS- and T-integral, the VG obtained using the Kors matrix was positioned more superior. The INVD derived VGx (36 ± 27 mV·ms) was significantly smaller as compared to the Kors derived VGx (39 ± 25 mV·ms). Overall, the difference in VGx between both matrices was small, however a large variation was observed (Figure 2D). The correlation coefficient of the VG magnitude obtained

by the INVD matrix and Kors matrix was 0.96 (*P*<0.001) and the correlation coefficient of the VGx obtained by the INVD matrix and Kors matrix was 0.97 (*P*<0.001).

The correlation between the SPAP and VCG parameters

In Table 3, the correlations between the VCG parameters and the SPAP, estimated with echocardiography, are summarized for both matrices. The correlations between on the one hand, the SPAP and, on the other hand, the magnitude and orientation of the QRS- and T-vector did not differ substantially between the INVD and Kors matrices, except for the QRS azimuth. The QRST spatial angle and the VG magnitude derived using the Kors matrix demonstrated a stronger correlation with the SPAP as compared to the INVD. The strongest correlation was found between the VGx and the SPAP, the correlation obtained using the INVD matrix (R=-0.48, p<0.001) was similar to the correlation obtained using the Kors matrix (R=-0.50, p<0.001).

Table 3. Correlations between systolic pulmonary arterial pressure on echocardiography and vectorcardiographic parameters

	INVD, R estimated SPAP	***P*-value**	**Kors, R estimated SPAP**	**Paired T-test *P*-value**
QRS mean (μV)	0.005	0.96	0.03	0.78
QRS axis azimuth (°)	-0.09	0.30	-0.23	0.008
QRS elevation (°)	0.02	0.79	-0.03	0.71
QRS integral (mV*ms)	0.04	0.69	0.05	0.59
T mean (μV)	-0.22	0.01	-0.24	0.006
T axis azimuth (°)	0.33	<0.001	0.24	0.007
T axis elevation (°)	-0.05	0.55	-0.14	0.10
T integral (mV*ms)	-0.21	0.02	-0.21	0.01
QRS-T angle (°)	0.18	0.04	0.33	<0.001
Ventricular gradient magnitude (mV*ms)	-0.30	0.001	-0.38	<0.001
Ventricular gradient azimuth (°)	0.30	0.001	0.16	0.06
Ventricular gradient elevation (°)	-0.01	0.88	-0.02	0.83
VGx (mV*ms)	-0.48	<0.001	-0.50	<0.001

INVD, inverse Dower matrix; VGx, ventricular gradient projected on the x-axis

Diagnosis of elevated pulmonary pressures by VGx

ROC curve analysis was performed to investigate the difference in diagnostic accuracy of the VGx for the presence of elevated pulmonary pressures, SPAP ≥ 36 mm Hg and SPAP ≥ 50 mm Hg, between the INVD and Kors matrices. The VGx synthesized by the INVD matrix yielded an AUC of 0.74 for the presence of SPAP ≥36 mm Hg and the VGx, synthesized using the Kors matrix, also showed an AUC of 0.74. (Figure 3A). Furthermore, the VGx synthesized by the INVD matrix demonstrated a comparable AUC for the presence of SPAP ≥ 50 mm Hg with the VGx synthesized by the Kors matrix (0.80 vs. 0.80, respectively, *P*=0.99; Figure 3B). To assess the association between both matrices and the presence of elevated SPAP of ≥ 36 mm Hg and ≥ 50 mm Hg, logistic regression analysis was performed. This analysis demonstrated that the VGx synthesized by INVD and Kors both provided

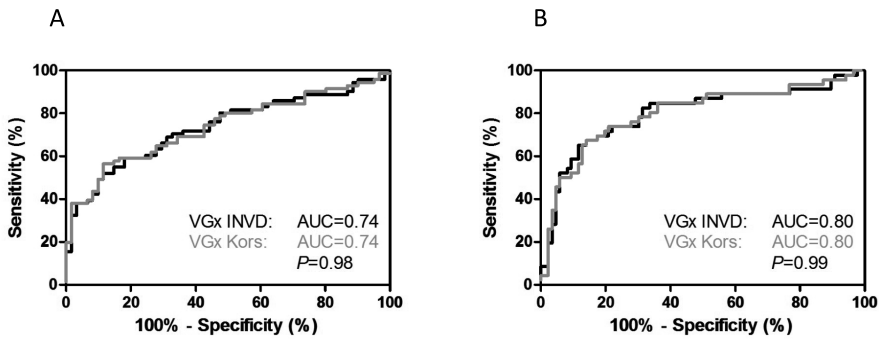

Figure 3. Receiver operator characteristic (ROC) curves for the detection of elevated pulmonary pressures, a systolic pulmonary arterial pressure ≥ 36 mm Hg (A) and ≥ 50 mm Hg (B) estimated with echocardiography, by VGx. AUC: area under the curve; VGx: ventricular gradient projected on the x-axis; INVD: inverse Dower matrix; KORS: Kors matrix.

significant diagnostic information on the presence of SPAP ≥ 36 mm Hg (odds ratio 1.04, 95%CI 1.02 – 1.05, *P*<0.001; odds ratio 1.04, 95%CI 1.02 – 1.05, *P*<0.001, respectively) and of SPAP ≥ 50 mm Hg (odds ratio 1.05, 95%CI 1.03 – 1.07, *P*<0.001; odds ratio 1.05, 95%CI 1.03 – 1.08, *P*<0.001, respectively; Table 4). Furthermore, patients with a reduced VGx (<24 mV*ms) by the INVD matrix, exhibited an odds ratio of 7.94 (95%CI 3.18 – 19.80, *P*<0.001) and patients with a reduced VGx by the Kors matrix, exhibited an odds ratio of 7.73 (95%CI 2.76 – 21.66, *P*<0.001) for the presence of SPAP ≥ 36 mm Hg. Moreover, the odds ratio for the presence of SPAP ≥ 50 mm Hg was 12.74 (95%CI 5.35 – 30.34, *P*<0.001) in patients with a reduced VGx by INVD and 8.29 (95%CI 3.45 – 19.93, *P*<0.001) in patients with a reduced VGx by Kors. After multivariate correction, the VGx synthesized by Kors and INVD remained significantly associated with the presence of elevated SPAP (Table 4).

DISCUSSION

The present study demonstrated that the synthesized VCG differed significantly in morphology between the INVD and Kors matrices. However, there was no significant difference between both matrices in clinical performance of the ECG-derived VGx in the detection of elevated SPAP on echocardiography.

The VCG outperforms the 12-lead ECG in the diagnosis of PH.[4] However in clinical practice, the 12-lead ECG is still most widely used.[7] This is probably because recording of an original VCG requires that the electrodes of the VCG are placed in a non-standard order with high precision on the designated location, rendering it a relatively cumbersome and slow technique.[19] Consequently, multiple conversion matrices have been developed to synthesize a VCG from the 12-lead ECG.

The INVD and Kors matrices defined how the x, y, and z deflections of a VCG can be derived from a standard 12-lead ECG. In these equations, the eight independent ECG leads (I, II, V1-V6) were multiplied by a lead specific value (coefficient) and added together to calculate one of the deflections of the VCG. The coefficient of a specific lead differs for each deflection (x, y or z).[7] The coefficients can be conceived in several ways. Edenbrandt et al. developed the INVD by inversing the Dower matrix.6 The Dower matrix was first introduced to synthesize

Table 4. Logistic regression analysis to predict the presence of elevated pulmonary pressures using the ventricular gradient

	Univariable analysis		Multivariable analysis*	
	OR (95% CI)	***P*-value**	**OR (95% CI)**	***P*-value**
SPAP >36 mm Hg				
INVD				
VGx (mV*ms)	1.04 (1.02 – 1.05)	<0.001	1.03 (1.02 – 1.05)	<0.001
VGx <24 mV*ms	7.94 (3.18 – 19.80)	<0.001	7.81 (2.99 – 20.44)	<0.001
KORS				
VGx (mV*ms)	1.04 (1.02 – 1.05)	<0.001	1.04 (1.02 – 1.06)	<0.001
VGx <24 mV*ms	7.73 (2.76 – 21.66)	<0.001	7.95 (2.70 – 23.46)	<0.001
SPAP > 50 mm Hg				
INVD				
VGx (mV*ms)	1.05 (1.03 – 1.07)	<0.001	1.05 (1.03 – 1.08)	<0.001
VGx <24 mV*ms	12.74 (5.35 – 30.34)	<0.001	12.35 (5.05 – 30.17)	<0.001
KORS				
VGx (mV*ms)	1.05 (1.03 – 1.08)	<0.001	1.05 (1.03 – 1.07)	<0.001
VGx <24 mV*ms	8.29 (3.45 – 19.93)	<0.001	8.19 (3.29 – 20.38)	<0.001

CI, confidence interval; INVD, inverse Dower matrix; OR, odds ratio; SPAP, systolic pulmonary arterial pressure; VGx, ventricular gradient projected on the x-axis
*Multivariable analysis corrected for age, gender and heart rate

a 12-lead ECG from the x, y and z deflections of the VCG.[9] The coefficients in de Dower matrix were based on the Frank's torso model.[19] Consequently, the coefficients in the INVD were the result of the inversion of the Frank's torso model based coefficients. The coefficients of the Kors matrix were the result of a statistical regression, aimed at optimizing the resemblance between the Frank VCG and the VCG synthesized from a simultaneously recorded ECG.[7] The VCG computed by Kors resembled the Frank VCG the most as compared to the other matrices. The coefficients of INVD and Kors are different and therefore it is evident that the matrices synthesize morphological different VCG's.

In the current study, the differences in morphology between the VCG obtained using the INVD matrix and the VCG obtained using the Kors matrix were assessed by comparing various VCG variables. A significant difference was observed between both matrices in the majority of the VCG parameters, which define the magnitude of a vector. The integral of the INVD-derived QRS-vector was significantly larger as compared to the integral of the Kors-derived QRS-vector, while there was no difference in the integral of the T-vector between both matrices. However, the VG, the resultant vector of the integrals of the QRS- and T-vector, was smaller when derived using the INVD matrix as when derived using the Kors matrix. The spatial QRST-angle, the angle between the QRS- and T-vector, was significantly wider in the VCG synthesized by the INVD matrix as compared to the VCG synthesized by the Kors matrix. Therefore, the wider spatial QRST-angle in the INVD reconstructed VCG caused the VG derived by the INVD to be lower as compared to the VG derived by the Kors matrix. Consequently, the distribution of the differences between both matrices for the individual VCG parameters are partially corrected in the combined VCG parameters, e.g. the VG and the VGx.

In addition, the inverse correlation between VGx and SPAP, estimated with echocardiography, was equal for both matrices. Subsequently, the described differences in morphology between INVD derived VCG and Kors derived VCG did not influence the correlation between VGx and SPAP, which is the relevant correlation for the clinical application of the ECG-derived VCG in patients suspected of PH.

Several studies compared methods for reconstructing the original VCG from the standard 12-lead ECG.[6,7] Kors et al. showed a difference in the cumulative distribution of numerical distances between three VCGs synthesized by respectively the INVD, Kors and a quasi-orthogonal matrix in a population, which predominantly consisted of a group of healthy subjects and a group of patients with myocardial infarction and patients with hypertrophy.[7] In this study, the INVD and Kors matrices were equal in diagnostic performance as compared to the original VCG, and were preferable to the quasi orthogonal matrix, which performance was less compared to the other two methods.[7] Similarly, Edenbrandt et al compared visually three different synthesized VCGs (the INVD, a method described by Bjerle et al.[20] and a method implemented by Marquette Electronics Inc (Milwaukee, WI) to the Frank VCG to determine which method resulted in the most comparable Frank QRS loop in a mixed population of normal controls and patients with myocardial infarction and right ventricular hypertrophy. The authors found that the INVD matrix showed the best method of synthesis in comparison to the other two methods.[6]

In line with the above mentioned studies, the current study observed that, despite the differences in morphology between the two methods, both matrices constructed a VCG that demonstrated equal clinical performance in patients with suspected PH.

Clinical implications

Early detection of PH is important in order to improve prognosis.[1-3] Therefore, simple and widely available diagnostic tests to detect PH are needed. Henkens et al. demonstrated that the ECG-derived VCG is accurate in the detection of elevated pulmonary pressures in idiopathic pulmonary arterial hypertension patients and healthy matched controls.[4] In addition, Scherptong et al. showed that the VCG is also of use for detection of elevated pulmonary pressures, for detection of PH and for mortality risk stratification, in a heterogeneous population suspected of PH.[5] Both authors used the INVD matrix.

In the present study, the difference in clinical performance of the VGx between the INVD and Kors matrices was assessed in a population of patients with suspected PH. First, the application of the VGx for the detection of elevated SPAP, estimated with echocardiography, was evaluated by ROC analysis, which showed almost identical AUC curves for both matrices. Therefore, the diagnostic accuracy of the VGx for elevated SPAP was equal between INVD and Kors. Secondly, the association between SPAP and the VGx was evaluated by logistic regression analyses for both matrices. This revealed similar odds ratios. Consequently, both matrices may be used to reconstruct a VCG for the clinical application of the VGx in patients suspected of PAH.

Limitations

In the present study, the VCG derived by the INVD matrix and the Kors matrix were not compared to the original VCG (Frank VCG). Therefore, the described morphological differences between INVD

and Kors were not absolute, but relative. However, this did not influence the comparison in clinical performance between both matrices, which was the main aim of the current study.

CONCLUSION

There is a significant difference in morphology of the vectorcardiogram between the INVD matrix derived VCG and the Kors matrix derived VCG in a population suspected of PH. However, the VCG synthesized by either the INVD matrix or Kors matrix demonstrate equal clinical performance in detecting elevated pulmonary pressures by VGx. Conclusively, the INVD and Kors matrices may both be used in a population evaluated for PH.

REFERENCES

1. Badesch DB, Raskob GE, Elliott CG et al. Pulmonary arterial hypertension: baseline characteristics from the REVEAL Registry. *Chest* 2010;137:376-87.
2. Brown LM, Chen H, Halpern S et al. Delay in recognition of pulmonary arterial hypertension: factors identified from the REVEAL Registry. *Chest* 2011;140:19-26.
3. Tueller C, Stricker H, Soccal P et al. Epidemiology of pulmonary hypertension: new data from the Swiss registry. *Swiss Med Wkly* 2008;138:379-84.
4. Henkens IR, Mouchaers KT, Vonk-Noordegraaf A et al. Improved ECG detection of presence and severity of right ventricular pressure load validated with cardiac magnetic resonance imaging. *Am J Physiol Heart Circ Physiol* 2008;294:H2150-7.
5. Scherptong RW, Henkens IR, Kapel GF et al. Diagnosis and mortality prediction in pulmonary hypertension: the value of the electrocardiogram-derived ventricular gradient. *J Electrocardiol* 2012;45:312-8.
6. Edenbrandt L, Pahlm O. Vectorcardiogram synthesized from a 12-lead ECG: superiority of the inverse Dower matrix. *J Electrocardiol* 1988;21:361-7.
7. Kors JA, van HG, Sittig AC et al. Reconstruction of the Frank vectorcardiogram from standard electrocardiographic leads: diagnostic comparison of different methods. *Eur Heart J* 1990;11:1083-92.
8. Dower GE. A lead synthesizer for the Frank system to simulate the standard 12-lead electrocardiogram. *J Electrocardiol* 1968;1:101-16.
9. Dower GE, Machado HB, Osborne JA. On deriving the electrocardiogram from vectoradiographic leads. *Clin Cardiol* 1980;3:87-95.
10. Galie N, Hoeper MM, Humbert M et al. Guidelines for the diagnosis and treatment of pulmonary hypertension: The Task Force for the Diagnosis and Treatment of Pulmonary Hypertension of the European Society of Cardiology (ESC) and the European Respiratory Society (ERS), endorsed by the International Society of Heart and Lung Transplantation (ISHLT). *Eur Heart J* 2009;30:2493-537.
11. Macfarlane PW, Devine B, Latif S et al. Methodology of ECG interpretation in the Glasgow program. *Methods Inf Med* 1990;29:354-61.
12. Draisma HHM, Swenne CA, van de Vooren H et al. LEADS: an interactive research oriented ECG/VCG analysis system. *Comput Cardiol* 2005;32:515-8.
13. Lepeschinin E, Surawicz B. The measurement of the Q-T interval of the electrocardiogram. *Circulation* 1952;6:378-88.
14. Kossman C, Brody D, Burch G. Report of committee on electrocardiography, American Heart Association. *Circulation* 1967;35:583-602.
15. Scherptong RW, Henkens IR, Man SC et al. Normal limits of the spatial QRS-T angle and ventricular gradient in 12-lead electrocardiograms of young adults: dependence on sex and heart rate. *J Electrocardiol* 2008;41:648-55.
16. Rudski LG, Lai WW, Afilalo J et al. Guidelines for the echocardiographic assessment of the right heart in adults: a report from the American Society of Echocardiography endorsed by the European Association of Echocardiography, a registered branch of the European Society of Cardiology, and the Canadian Society of Echocardiography. *J Am Soc Echocardiogr* 2010;23:685-713.
17. Bland JM, Altman DG. Statistical methods for assessing agreement between two methods of clinical measurement. *Lancet* 1986;327:307-10.
18. Hanley JA, McNeil BJ. A method of comparing the areas under receiver operating characteristic curves derived from the same cases. *Radiology* 1983;148:839-43.
19. Frank E. An accurate, clinically practical system for spatial vectorcardiography. *Circulation* 1956;13:737-49.
20. Bjerle P, Niklasson U. Comparison between three different stand-alone ECG interpretation systems. *J Electrocardiol* 1988;21 Suppl:S163-S168.